

# Identification of earthquake signals from groundwater level records using the HHT method

Chieh-Hung Chen,<sup>1</sup> Chung-Ho Wang,<sup>1</sup> Jann-Yenq Liu,<sup>2,3</sup> Chen Liu,<sup>4</sup> Wen-Tzong Liang,<sup>1</sup> Horng-Yuan Yen,<sup>5</sup> Yih-Hsiung Yeh,<sup>1</sup> Yee-Ping Chia<sup>6</sup> and Yetmen Wang<sup>7</sup>

<sup>1</sup>Institute of Earth Sciences, Academia Sinica, Taipei 115, Taiwan. E-mail: nonono@url.com.tw

<sup>2</sup>Institute of Space Science, National Central University, Chung-Li 32054, Taiwan

<sup>3</sup>Center for Space and Remote Sensing Research, National Central University, Chung-Li 32054, Taiwan

<sup>4</sup>Department of Civil Engineer, Dahan Institute of Technology, Hualien 971, Taiwan

<sup>5</sup>Institute of Geophysics, National Central University, Chung-Li 32054, Taiwan

<sup>6</sup>Department of Geosciences, National Taiwan University, Taipei 115, Taiwan

<sup>7</sup>ACD Co., Taiwan

Accepted 2009 December 3. Received 2009 December 3; in original form 2008 May 12

## SUMMARY

Coseismic signals of groundwater levels are generally obtained by subtracting the responses of atmospheric pressure, Earth tides and precipitation from the observed data. However, if the observations are conducted without nearby barometers, pluviometers or Earth tide data for correction, coseismic signals are often difficult to extract. In this case, the Hilbert–Huang transform (HHT) is used to obtain the instantaneous frequencies and amplitudes for every point of the decomposed intrinsic mode functions (IMFs) from groundwater level data for differentiating the related frequency-dependent responses without a further auxiliary input. The extracted coseismic signals show intense amplitude pulses that are clearly seen in the third IMF. In addition, two types of coseismic signals can be readily distinguished in the results from the HHT transform. One is an instantaneous short-time signal induced by the passing of seismic waves. Another coseismic signal is a sustained signal induced by the near-field earthquake occurring near the Hualien station, Taiwan and shows a positive correlation between the earthquake distance and magnitude. Our results generally show that using the HHT transform improves our understanding of automatic detection of the coseismic signals from the groundwater level.

**Key words:** Time-series analysis; Hydrology; Earthquake interaction, forecasting, and prediction.

## INTRODUCTION

The relationship between coseismic signals and groundwater level has intrinsic potential for understanding essential characteristics of an aquifer during earthquakes (Igarashi & Wakita 1991; Quilty & Roeloffs 1997; Roeloffs 1998). In general, variations of groundwater level are a composite result by responses of atmospheric pressure, Earth's tidal activity and precipitation (Bredehoeft 1967; Van der Kamp & Gale 1983; Narasimhan *et al.* 1984; Roeloffs 1988). During an earthquake event, coseismic signals of groundwater level are normally weak in the background and only for a very short appearance if recorded.

For extracting and retrieving weak earthquake signals from long-term groundwater variations, responses of atmospheric pressure and the Earth tides, which are two conspicuous intrinsic functions of the groundwater levels, have to be removed first. The least-squares regression analysis is the simplest method for estimating the

responses of atmospheric pressures and Earth tides in the coseismic signals by one or two single coefficients, respectively (Roeloffs 1988). However, Rojstaczer (1988) indicated that the responses of atmospheric pressure depended on the frequency for a poorly or partially confined aquifer; thus site effect is inherently important. Later, Quilty & Roeloffs (1991) characterized and removed the responses of the atmospheric pressures at subtidal frequency and Earth tides by frequency-dependent transfer functions with limited success. Note that the major frequencies of the atmospheric pressure and the Earth tide exhibit as 2 and 1 d<sup>-1</sup> in groundwater level records, respectively.

Alternately, coseismic signals are often disturbed by precipitation due to the short temporal period coinciding with that of atmospheric pressure and the Earth tide. Matsumoto (1992) applied a two-stage method to separate tide responses from coseismic signals of groundwater levels by a weighted sum during the entire observation period and obtained precipitation responses using an

impulse-response model. However, noise is still attached in the residual and affects the identification of earthquake signals. Kitagawa & Matsumoto (1996) illustrated that the groundwater level is composed of aforementioned three responses, a noise and a long-term trend component via a state-space representation. By noise reduction, Matsumoto & Roeloffs (2003a,b) were able to search the coseismic signals and successfully identified 28 earthquakes in the residual groundwater level record at the Haibara well in central Japan from 1981 to 1997. In short, groundwater level records have the potential to retrieve earthquake signals if other auxiliary observations such as barometers, pluviometers and Earth tide variations can be filtered out and/or separated from earthquake once after applying methods with substantial noise reduction. Thus, without the help of other auxiliary observations, coseismic signals are inherently recorded with groundwater level changes and cannot be extracted effectively.

In this study, we take advantage of high resolution groundwater level records (at two-minute interval) at the Hualien well (Fig. 1) in eastern Taiwan from 2004 to 2006 for a novel attempt to effectively separate earthquake signals from groundwater level changes without other auxiliary observations. In our approach, groundwater level records are first decomposed into many intrinsic mode functions (IMFs) via the empirical mode decomposition (EMD), and

their instantaneous frequencies and amplitudes are obtained using the Hilbert transform (HT) in a temporal period. The instantaneous frequencies are taken to compare with known characteristics of various tides associated with groundwater level variations and the residual can then be employed in identifying coseismic signals.

## THEORY AND METHODOLOGY

The atmospheric pressure and Earth's tide are frequency-dependent responses (Quilty & Roeloffs 1991) and time-series data of the groundwater level are thus transferred to a frequency domain for easy reduction. Traditionally, the Fourier Transform is used for filtering observed data to reveal the signals. Although the Fourier Transform has been developed with a sound mathematic theory, the adopted time-series data are assumed to be linear and stationary. Meanwhile, a low frequency is often a limiting factor for data continuity. In contrast, the Hilbert–Huang transform (HHT) can be employed in a non-linear or non-stationary data set, thus is used here for transferring the data into the frequency domain (Huang & Shen 2005).

The HHT process involves two primary steps, EMD and then HT. To obtain a subsequent better HT results, the EMD step plays

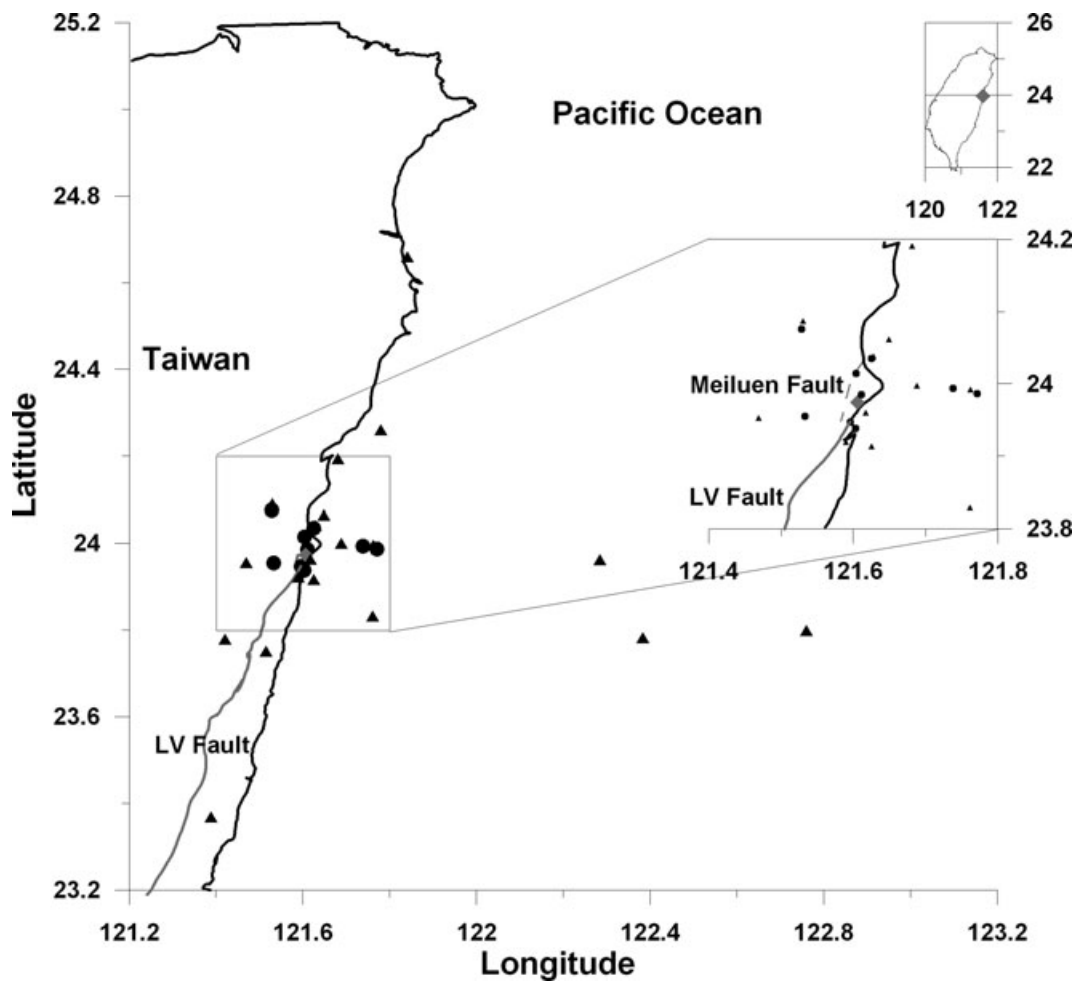


**Figure 1.** The location of the Hualien station (grey diamond) and the earthquake epicentres with observed coseismic signals (circle and triangle). The circle and triangle denotes type-A and B in the raw data, respectively. The earthquake epicentres are listed in Table 2. The dashed and shadow lines show Meiluen and LV faults located to the west and south of Hualien station, respectively.

an important role. Huang *et al.* (1998) indicated that the EMD was based on direct energy extraction associated with various intrinsic timescales, that is, the most important parameter of the data set to decompose the non-stationary and non-linear data into many IMFs. EMD is a shifting process of energy extractions to obtained IMFs. The input data series are first subtracted by means of top and bottom envelopes, which are constructed, respectively, by the local maximum and minimum of the input data (for detail, see Huang *et al.* 1998). Then, the obtained residual data are examined to determine whether they are IMFs or not. In this study, if the means of the obtained residual data are larger than  $10^{-3}$  m, they are adopted to substitute for the input data and repeat the shifting process. On the

other hand, if the mean is smaller than  $10^{-3}$  m, the shifting process is temporarily stopped and residual data are taken as an IMF. To obtain subsequent unknown IMFs, the data of the next shifting process are replaced by those from subtracting all obtained IMFs, and repeat the shifting process as above. The EMD process ends as the number of local maximum or minimum is less than 2. Based on these extractions, IMFs from high to low frequencies are generally obtained in sequence. Finally, the instantaneous amplitudes and frequencies at each observed point of IMFs can be obtained by the HT (Huang *et al.* 2003).

For example, a time-series data would yield  $j$  IMFs, using the  $X_j(t)$  of EMD and the  $Y_j(t)$  is given by the HT (Bedrosian 1963;

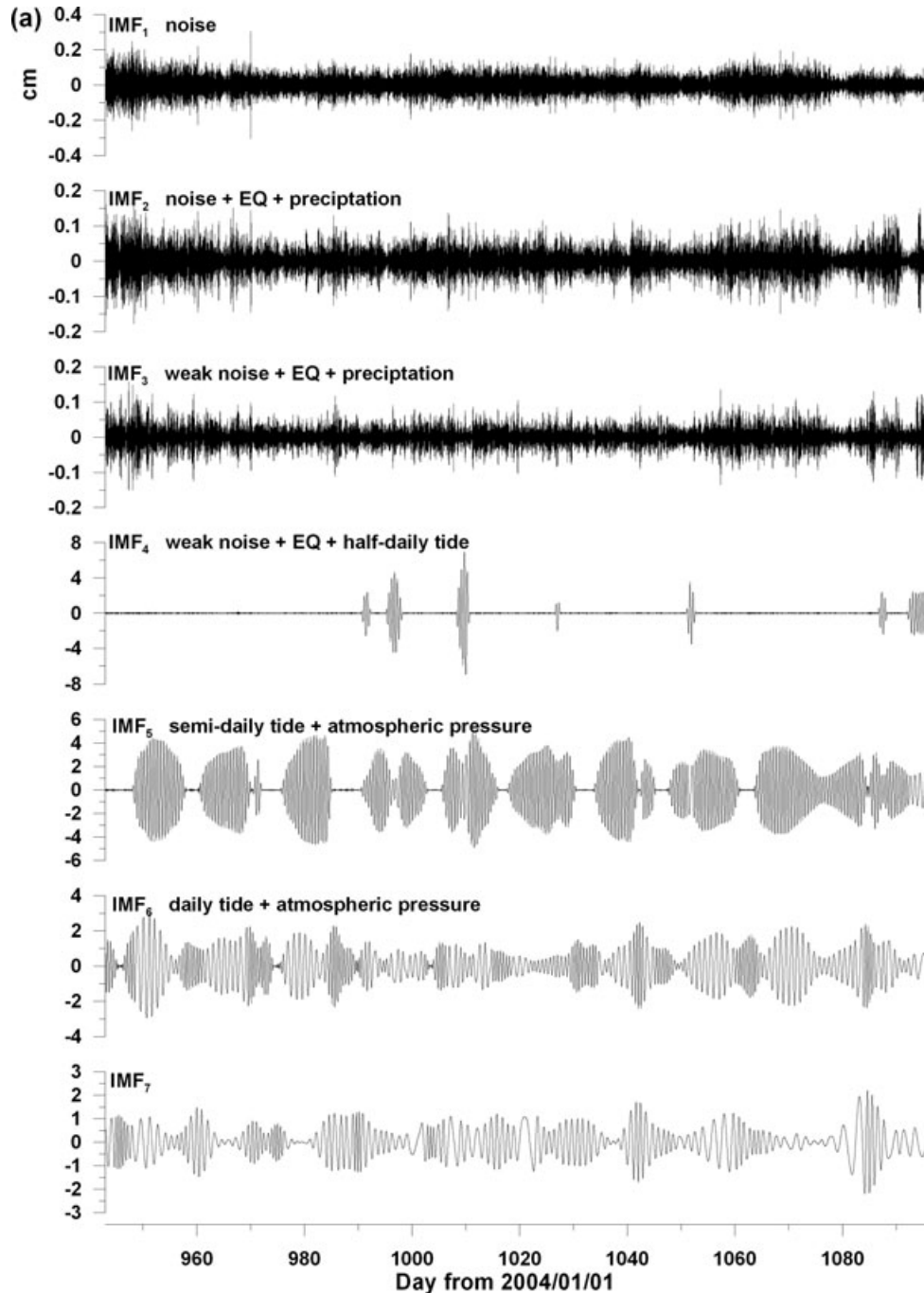


Figure 2. The IMFs of the groundwater level from 2006 July to December at the Hualien station.

Barnes 1992; Hahn 1996)

$$Y_j(t) = \frac{1}{\pi} P \int_{-\infty}^{\infty} \frac{X_j(s)}{t-s} ds,$$

where  $s$  is the integration variable and  $P$  is the Cauchy principal value. The analytic signal,  $Z_j(t)$ , is defined as

$$Z_j(t) = X_j(t) + iY_j(t) = a_j(t)e^{i\theta(t)},$$

where

$$a_j(t) = [X_j^2(t) + Y_j^2(t)]^{1/2} \quad \text{and} \quad \theta_j(t) = \arctan \left[ \frac{Y_j(t)}{X_j(t)} \right].$$

Here  $a(t)$  is the instantaneous amplitude,  $\theta(t)$  is the phase function, and the instantaneous frequency ( $\omega$ ) is simply as

$$\omega = \frac{d\theta_j(t)}{dt}.$$

Therefore, a time-series records of the groundwater level can be analysed using HHT method and separated into many IMFs.

In this work, the Hualien groundwater level data were first analysed after a low pass filter for removing noises. Nevertheless, it is difficult to prove that the filtered data still contained the needed signals entirely. Thus, the groundwater level records were directly analysed by every observed point taking the HHT as HHT<sub>1</sub>.

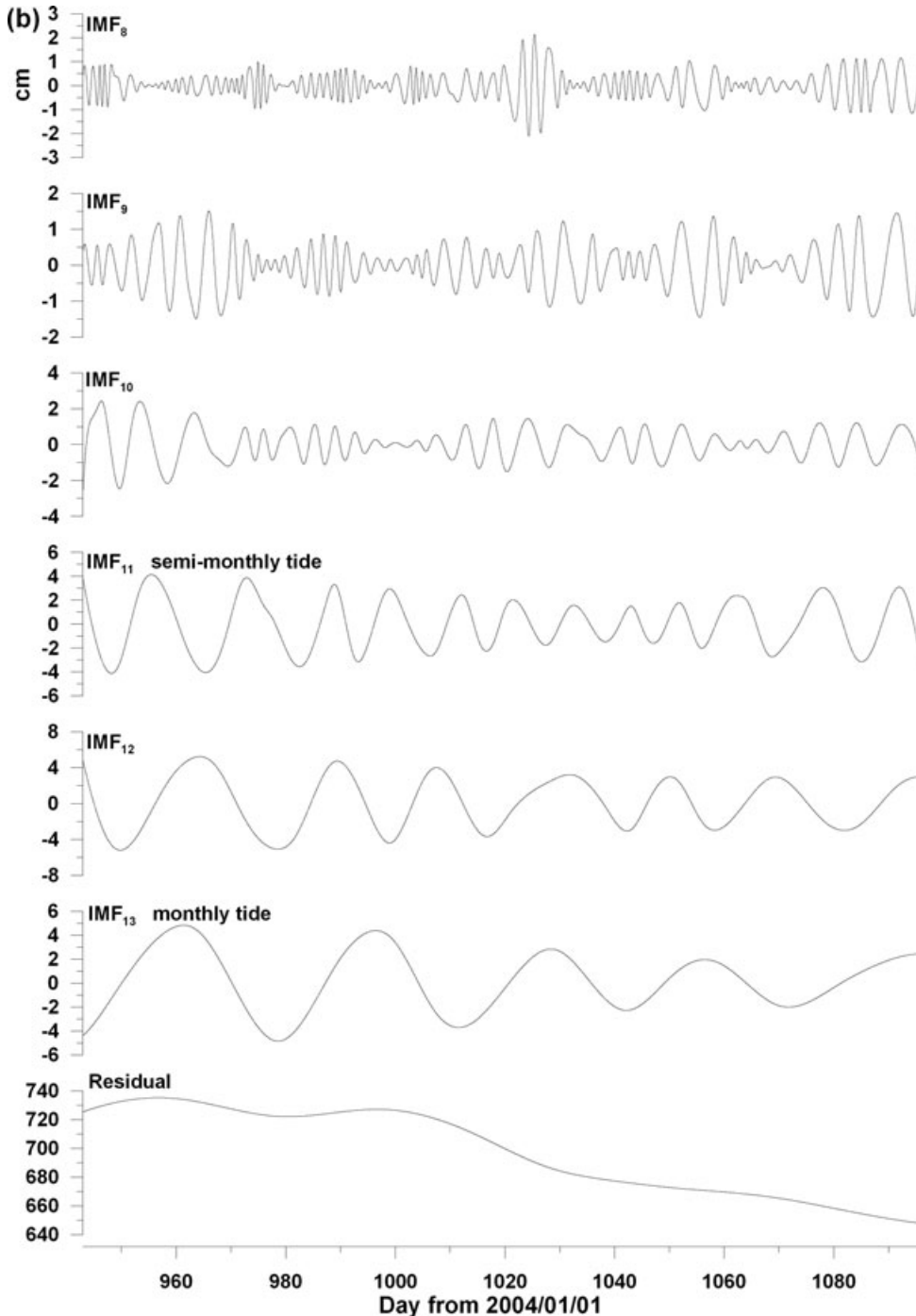


Figure 2. (Continued.)

Instead of using low pass filter, we reconstruct the other two time-series data designated as HHT<sub>2</sub> and HHT<sub>3</sub> with a down-scale of every 2 (4 min) and 3 (6 min) observed points from recorded data (HHT<sub>1</sub>), respectively, to detect long-term changes associated with earthquakes and to reduce simultaneously the disturbance from high frequency noises. Note that *dt* changes to 240 s for HHT<sub>2</sub> and 360 s for HHT<sub>3</sub> accordingly.

Due to the hardware limitation, the data were cut by less than 200 000 observed points for HHT process. The instantaneous amplitude and frequency of each point in *j* IMFs (IMF<sub>*j*</sub>) can be obtained. After frequency comparisons between the IMF<sub>*j*</sub> and the known responses, IMFs associated with semi-daily, daily, and monthly tides can be distinguished. The other IMFs are further engaged to relate with earthquakes.

Effects of coseismic signals are generally observed during a relative short temporal period. IMFs with the frequencies lower than the semi-daily tide (2 1 d<sup>-1</sup>) are first eliminated from our consideration. On the other hand, IMFs with small instantaneous amplitudes and high frequencies are considered as noises. In the end, IMFs with median instantaneous frequencies, which are higher than 2 1 d<sup>-1</sup> and lower than noises, are used to compare with the earthquake catalogue. The obtained instantaneous amplitudes describe the energy variations and are treated as assistant parameters for determining the timescale of the related events. Taking the same data set of this study, we also examine the relationship between hypocentre distances and magnitudes of earthquakes in the coseismic signals.

**OBSERVATION AND INTERPRETATION**

Taiwan is located in the western side of the circum-pacific seismic zone and a complex boundary between the Eurasian and the Philippine Sea plates (Ho 1988). The Philippine Sea Plate moves northwest towards the Eurasian Plate with a rate of 70 km Myr<sup>-1</sup> that has resulted in two collision zones on the island with numerous earthquakes. The Longitudinal Valley fault (LV fault), one of the collision zones on land, is located in the eastern part of Taiwan and closely related with the active Meiluen fault (ML fault) found at the northwestern side of the LV fault (Fig. 1). To monitor the groundwater level response affected by these two fault systems during earthquake events, the Hualien Well (23.974°N, 121.606°E, located at the southern and northern end of the ML and LV faults, respectively; sampling rate = 2 min) was set-up and equipped with barometer and pluviometer (Fig. 1) since 2004. The high-resolution groundwater level data of Hualien Well were analysed from 2004 to 2006 in order to explore its relation with local earthquakes. Because this study is focused on the responses of coseismic signals from groundwater level variations, earthquake locations should be retrieved as precisely as possible. Locations of earthquakes are obtained from the catalogue of the Central Weather Bureau (CWB) in Taiwan. One of the major factors that induces significant variations on the groundwater level and cannot be neglected in this study is the impact of typhoons, which exhibit characteristics of very low atmospheric pressure, heavy rainfall and strong wind. Typhoons are normally prevalent from May through November during the southwesterly monsoon season in Taiwan. Similarly, the characteristics of typhoons are also obtained from CWB catalogue of Taiwan (<http://rdc28.cwb.gov.tw/>).

Due to no data in July, Figs 2(a) and (b) show IMF<sub>*j*</sub> of HHT<sub>3</sub> from 2006 August to December, and their median periods are listed in Table 1. In the HHT processing, IMF<sub>1</sub> with the instantaneous median frequency of 22.222 1 d<sup>-1</sup> is first separated from the Hualien

**Table 1.** The median periods and their descriptions of IMFs found in Fig. 2.

IMFs	Median frequency (1 d <sup>-1</sup> )	Signals (EQ = earthquake)
1	22.222	Noise
2	20.408	Noise + EQ + precipitation
3	26.954	Weak noise + EQ + precipitation
4	15.337	Weak noise + EQ + half-daily tide
5	1.957	Half-daily tide + atmospheric pressure
6	1.139	Daily tide + atmospheric pressure
7	0.809	
8	0.481	
9	0.266	
10	0.158	
11	0.077	Half-monthly tide
12	0.045	
13	0.031	Monthly tide

groundwater data. IMF<sub>1</sub> with very high frequency and small energy is considered as a noise component. IMF<sub>2</sub> with a frequency (20.408 1 d<sup>-1</sup>) close to the IMF<sub>1</sub> suggests that this component also carries primarily the noise. It is interesting to note that the IMF<sub>3</sub> has the highest frequency (26.954 1 d<sup>-1</sup>) with several large-amplitude peaks. The high frequency of IMF<sub>3</sub> may be continuously transmitted from noise that has the primary energy and is easily extracted from the record data. Coseismic signals that intermittently affect the groundwater levels have secondary energy and are extracted from the data in this component.

For IMF<sub>4</sub>, most data have small amplitudes at a high frequency range and are similar to IMF<sub>1-3</sub>. However, a few points in IMF<sub>4</sub> with large amplitudes at the low frequency range are related with IMF<sub>5</sub>. These large peaks in IMF<sub>4</sub> are considered as the energy leakage from IMF<sub>5</sub> due to the high similarity between their amplitudes and frequencies. The IMF<sub>5</sub> and IMF<sub>6</sub> with frequencies of 1.957 and 1.139 1 d<sup>-1</sup>, respectively show the variations of half and daily tides in the groundwater level records, along with atmospheric pressure. After separating the high frequency data in IMF<sub>*j*</sub> (*j* = 1–6), the frequency, which is lower than 1 1 d<sup>-1</sup>, is obtained in IMF<sub>*m*</sub>, (*m* = 7–13). In particular, the semi-monthly and monthly tides are shown in IMF<sub>11</sub> and IMF<sub>13</sub>, respectively. The last residual is illustrated in the bottom of Fig. 2(b), and represents the long-term decreasing trend of Hualien groundwater level.

The frequency range of the coseismic signals is generally lower than those of the semi-daily tide, and are involved in IMF<sub>*j*</sub>, (*j* = 1–4). In IMF<sub>1</sub> and IMF<sub>2</sub>, strong noises dominate the time-frequency diagrams and IMF<sub>4</sub> carries some long-period signals from IMF<sub>5</sub>. Thus, IMF<sub>3</sub> is the best candidate for identification. However, it does not warrant finding that the median instantaneous frequency of IMF<sub>3</sub> is lower than IMF<sub>2</sub>, and is inconsistent to the normal EMD process. To account for this inconsistency, the variations of atmosphere pressure, groundwater level, precipitation and typhoon events are compared with IMF<sub>3</sub> for HHT<sub>1</sub>, with the associated IMFs for HHT<sub>2</sub> and HHT<sub>3</sub> from 2004 to 2006 (Figs 3–5). The HHT<sub>1</sub>, HHT<sub>2</sub> and HHT<sub>3</sub> represent the results from different sampling rates during the data processing (HHT<sub>1</sub> = every 1 point; HHT<sub>2</sub> = every 2 points and HHT<sub>3</sub> = every 3 points). Table 2 lists the peaks associated IMFs in the columns of HHT<sub>*i*</sub>, (*i* = 1, 2, 3) (numbers 1 and 0 of that column indicate the groundwater level with or without strong peaks at a specific event, respectively). It is apparent that intense peaks are closely related to major earthquakes (Table 2; locations are shown in Fig. 1) and strong typhoons (solid triangles in Figs 3c, 4c and 5c).

**Table 2.** The numbered peaks of strong amplitudes in Fig. 3. Related source and the raw data types are also shown. HD denotes the hypocentre distance from the earthquake hypocentre to the Hualien well. The 1 and 0 shown in the column of  $HHT_i$  describe that the groundwater level with and without the numbered strong peaks at numbered time, respectively. The R.T. means the correlated the raw data type-A/B shown in Fig. 6. Note that the occurrence time of no. 23–1 is too close no. 23 to separate in Fig. 4 and we detect it in the computer via a small scale.

No.	Date	Lat. (°)	Long. (°)	Depth (km)	$M_L$ (km)	HD	$HHT_i$			R.T.
							$i = 1$	$i = 2$	$i = 3$	
1	2004/01/13	23.9866	121.771	4.81	4.78	17.51	1	1	1	A
2	2004/02/09	23.9913	121.762	33.17	3.96	36.82	1	1	1	B
3	2004/02/20	23.7780	122.383	9.16	4.12	82.45	1	0	0	B
4	2004/02/24	23.7475	121.515	58.51	4.72	64.32	1	0	0	B
5	Unknown disturbance						1	0	1	B
6	2004/04/24	23.9518	121.469	16.51	4.94	21.74	1	0	0	B
7	2004/05/01	24.0758	121.528	21.55	5.25	25.58	1	1	1	A
8	2004/07/22	24.0853	121.530	22.01	4.61	26.38	1	0	0	B
9	Data gap									
10	2004/11/08	23.7948	122.760	10.00	6.58	119.44	1	1	0	B
11	2004/11/13	23.9960	121.688	29.55	4.28	30.80	1	0	1	B
12	Unknown disturbance						1	1	1	B
13	2005/02/01	24.2558	121.780	5.74	5.14	36.31	1	0	0	B
14	2005/03/05	24.6546	121.841	6.39	5.90	79.26	1	1	0	B
15	2005/04/05	24.0600	121.649	7.80	3.98	13.06	1	0	1	B
16	2005/04/30	24.0351	121.625	8.45	5.62	10.99	1	1	1	A
17	2005/05/04	24.0143	121.604	8.97	4.78	10.01	0	1	1	A
18	2005/05/13	24.0373	121.628	8.90	4.61	11.54	1	1	1	B
19	2005/06/05	23.9471	121.596	5.65	4.16	6.47	1	1	1	A
20	2005/06/07	23.9933	121.738	2.09	5.16	13.75	1	1	1	A
21	2005/06/10	23.9383	121.603	7.55	4.85	8.53	1	1	1	A
22	2005/06/13	23.9121	121.625	23.36	4.59	24.42	1	0	0	B
23	2005/06/16	23.9590	121.617	7.75	4.19	8.00	1	1	1	B
23–1	2005/06/18	23.9546	121.533	2.18	5.00	8.02	1	1	1	A
24	2005/06/28	23.9181	121.590	4.39	3.95	7.76	1	0	0	B
25	Typhoon						1	1	1	
26	2005/07/31	24.1898	121.681	34.35	4.82	42.52	1	1	0	B
27	Typhoon						0	1	1	
28	Typhoon						1	1	1	
29	2005/09/06	23.9581	122.284	16.76	6.00	70.98	1	0	0	B
30	Typhoon						1	1	1	
31	Typhoon						1	1	1	
32	Unknown disturbance						0	1	0	B
33	Data gap									
34	Data gap									
35	Data gap									
36	Unknown disturbance						1	0	0	B
37	2006/04/28	23.9853	121.611	9.78	5.21	9.87	1	1	1	A
38	Data gap									
39	Data gap									
40	Data gap									
41	2006/10/08	23.7743	121.421	28.93	4.28	40.98	1	0	0	B
42	2006/12/06	23.8278	121.761	43.71	4.53	49.20	1	0	0	B
43	2006/12/26	23.3641	121.388	15.09	4.51	72.62	1	0	0	B

The variations of plots (a) and (b) in Figs 3–5 can be easily identified by the concurrent atmosphere pressure abrupt-drop and groundwater level rise. For example, effect of a typhoon with very low atmosphere pressure and heavy rainfall can be visible in the groundwater level on the 182th day from 2004 January 1 (Figs 3a–c). Effects of typhoons can be observed in all plots of  $HHT_1$ ,  $HHT_2$  and  $HHT_3$ , because the groundwater level takes a longer time to reduce their intense inputs.

After the identification of typhoon peaks, the intense signals related to earthquakes can then be separated by the sampling rating of 240 s (4 min) and 360 s (6 min), respectively (Figs 3e, f, 4e, f, 5e and f). A further careful examination of earthquake effects on Hualien groundwater level records in the deduced data set, two responsive

types can be distinctly recognized (Fig. 6). Type-A illustrates that the groundwater level suddenly dropped when the earthquake occurred with a short hypocentre distance (HD) such as the case of No. 1 in Table 2 (17.51 km on 2004 January 13) and yielded an off-trend displacement (Fig. 6a). When the disturbed material becomes stable, the displacement was stopped. The original tidal variation resumed again 1 hr later (Fig. 6a). Thus, type-A can be readily found in the low sampling rate  $HHT_3$ , because this kind of coseismic signals is generally longer than 6 min. On the other hand, type-B shows just one brief leap in the groundwater level time-series when the earthquake occurred, as exemplified in No. 3 of Table 2 (2004 February 20). Type-B can only be found in the high sampling rate  $HHT_1$  and should be identified very carefully due to its short and

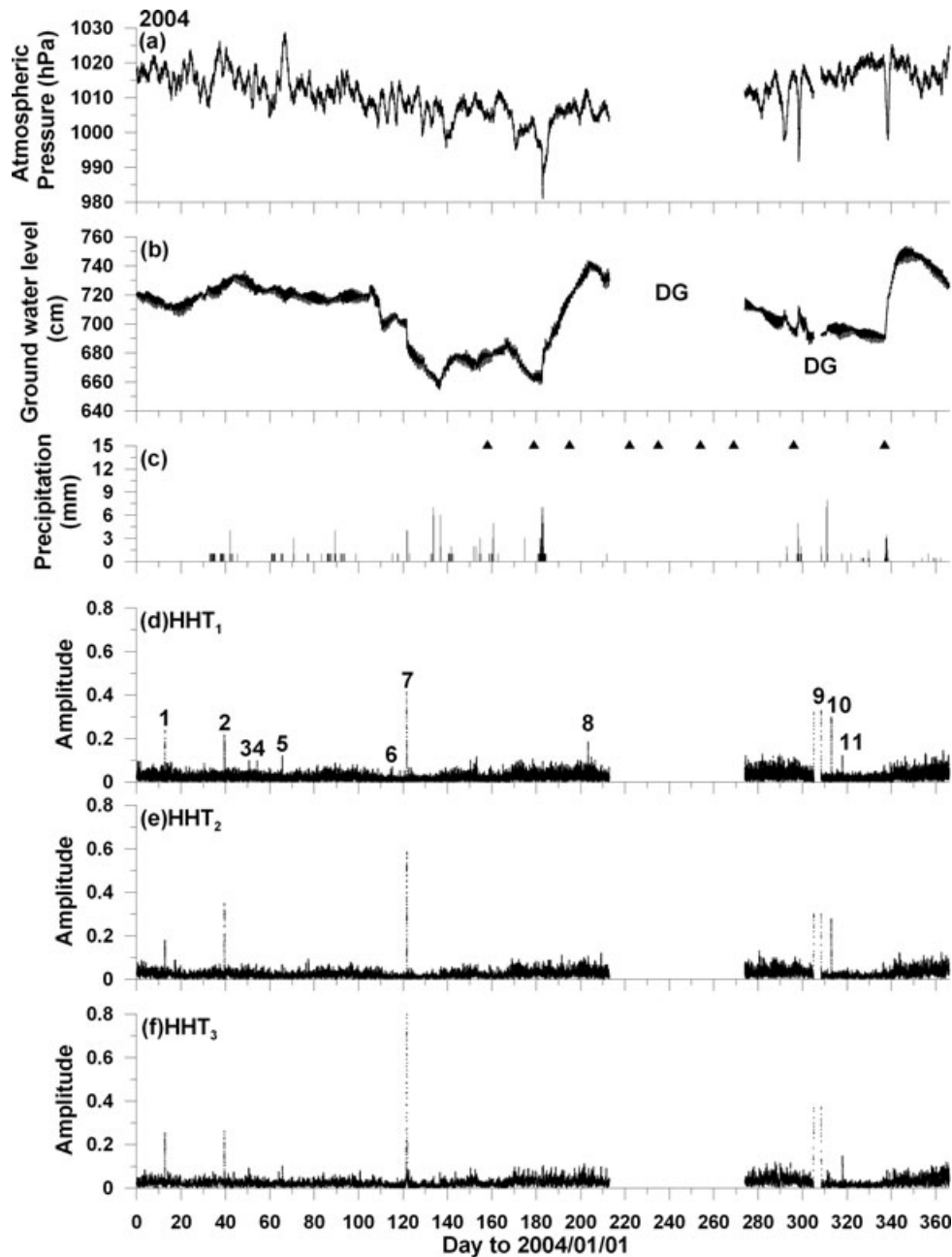


**Figure 3.** The variation of the atmospheric pressure, groundwater level, typhoons, precipitation and IMF<sub>3</sub> amplitudes of the HHT<sub>1</sub>, HHT<sub>2</sub> and HHT<sub>3</sub> in 2004. The DG denotes the data gap in the atmospheric pressure and the groundwater level time-series. The strong peaks of the IMF<sub>3</sub> amplitudes which are possibly related with earthquake coseismic changes are numbered in Table 2.

sharp response. In some cases, unknown disturbances can generate the same feature as shown in Table 2 and Figs 3–5 (#5, #12, #32 and #36). All the earthquake signals on Hualien groundwater level from 2004 to 2006 are classified as either type-A or B and compiled in the last column of Table 2. In addition, frequencies of type-A and/or type-B in Hualien well mainly ranged between about 12 and 34  $\text{d}^{-1}$ .

The relationship between the earthquake magnitudes and HD in Types A and B responses is further investigated. Fig. 7 exhibits the correlation between the magnitudes and HD of all earthquakes with and without coseismic signals in the Hualien groundwater level records. The dashed line represents the lower limit for 286 earthquakes ( $M_L \geq 3.95$ ;  $\text{HD} \leq 120$  km) without coseismic signals

(open circles in Fig. 7). A total of 28 coseismic events were observed in the Hualien groundwater level records from 2004 to 2006, nine of them belong to type-A and nineteen to type-B. Our results are compatible with the previous study that showed the threshold relationship between distance from epicentre (or hypocentre) versus earthquake magnitude for seismically induced changes in well levels or groundwater-controlled springs (Montgomery & Manga 2003). It is evident that all type-A events have a common characteristics of relatively short HD ( $\text{HD} = 6.47\text{--}25.58$  km) that is proportional to their magnitudes, as compared to type-B peaks with relatively broad HD ranges ( $\text{HD} = 7.76\text{--}119.44$  km). Furthermore, all type-A events distribute exclusively on the left side of the dashed line in Fig. 7 and type-B events crossover the boundary but

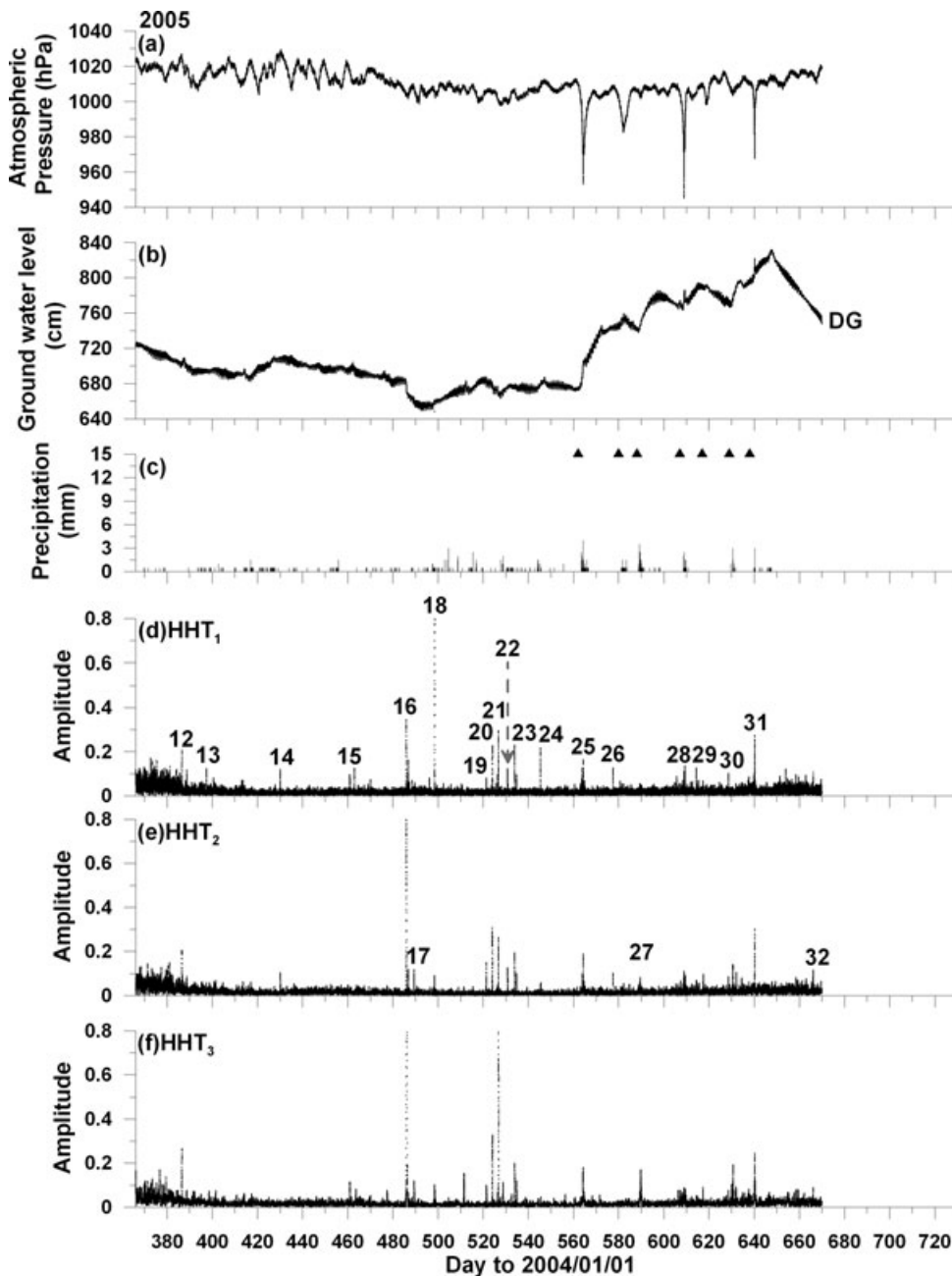


**Figure 4.** The variation of the atmospheric pressure, groundwater level, typhoons, precipitation and IMF<sub>3</sub> amplitude of the HHT<sub>1</sub>, HHT<sub>2</sub> and HHT<sub>3</sub> in 2005. The DG denotes the data gap in the atmospheric pressure and the groundwater level time-series. The strong peaks of the IMF<sub>3</sub> amplitudes which are possibly related with earthquake coseismic changes are numbered in Table 2.

primarily on the right-hand side. The discrepancy between types A and B in Fig. 7 is very interesting and implies that it is caused by different mechanisms from earthquakes. A detailed study is suggested to further analyse this important phenomenon.

## DISCUSSION AND CONCLUSIONS

This study has also tried to focus on the relationship between earthquake magnitudes versus epicentre distances in discussing groundwater level variations. However, as shown in Fig. 1, neither type-A nor type-B signals can be differentiated with each other by epicentre distances. On the contrary, both types can be readily separated using HD instead as demonstrated in Fig. 7. This unique feature of

Fig. 7 suggests that the characteristics between the type-A and B are quite different. In general, the type-B event is primarily observed at HHT<sub>1</sub>, but often missed at HHT<sub>2</sub> and HHT<sub>3</sub> (Figs 3–5). Thus, the appearance period of type-B is generally less than 2 min (the sampling rate of Hualien monitoring well) cannot be fully observed at lower sampling rate analysis (>2 min). On the other hand, many studies have shown that when the earthquake seismic wave propagations pass through and result the strain changes near the well, the groundwater levels are often disturbed within a short temporal period (Brodsky *et al.* 2003; Kano & Yanagidani 2006; Doan & Cornet 2007). Based on the changes without off-trend disturbance, type-B signals are elastic responses of medium caused by the continuous variations for the tides with long-term period.

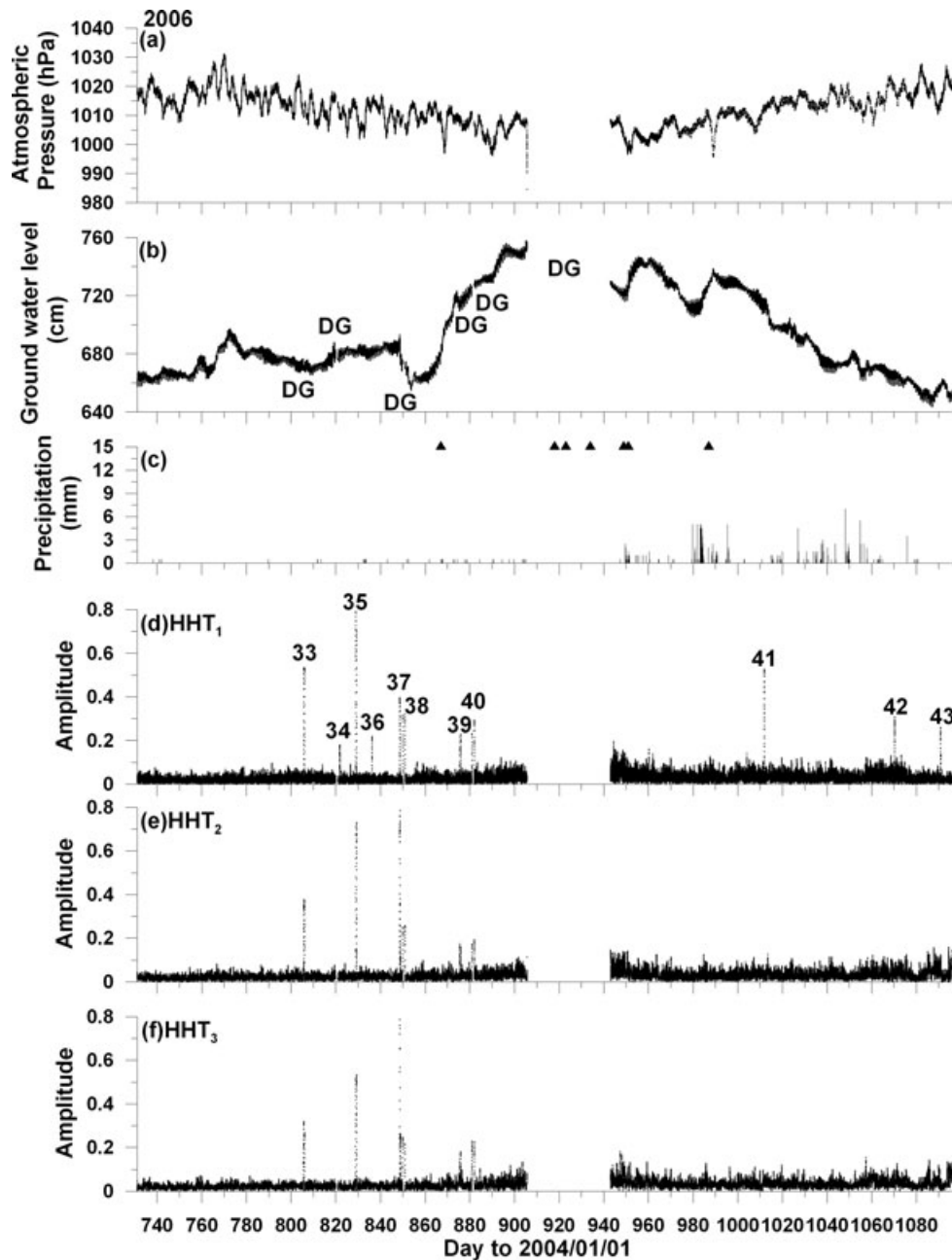


**Figure 5.** The variation of the atmospheric pressure, groundwater level, typhoons, precipitation and IMF<sub>3</sub> amplitudes of the HHT<sub>1</sub>, HHT<sub>2</sub> and HHT<sub>3</sub> in 2006. The DG denotes the data gap in the atmospheric pressure and the groundwater level time-series. The strong peaks of the IMF<sub>3</sub> amplitudes which are possibly related with earthquake coseismic changes are numbered in Table 2.

The ratio of observed type-B peaks in HHT<sub>3</sub> versus HHT<sub>1</sub> plus HHT<sub>2</sub> is 5/19 (= 26.3%), and approaches the occurrence probability (33%) as the down-scale data sampling (HHT<sub>3</sub>) by every three observed points from HHT<sub>1</sub>. Hence, the observation of type-B signals in the Hualien groundwater records is mainly caused by the arrival of strong seismic waves. On the other hand, the type-A signals observed in the Hualien groundwater records exhibit not only a coseismic variation but also last for a certain period to get the groundwater level back to the normal trend (Fig. 6). The obvious discrepancy between types A and B in the Hualien records strongly suggests that the mechanisms are very different in terms of groundwater response to the arrival of seismic waves. In cases of type-A response, HD are positively correlated to their respective

earthquake magnitudes, and confined to the left side of distribution limit defined by earthquakes without coseismic signals in the Hualien groundwater records (Fig. 7). This feature may be related to the fault geometry, intensity coverage and strain change during the earthquake events.

In previous studies, to observe the type-A coseismic signals in the groundwater level variations during an earthquake, parameters of the barometers, pluviometers and variations of the Earth tide are all required. In this work, we demonstrate that using HHT analyses for the groundwater level record, we can directly achieve the same or even better results. By the HHT method, many major sources can be clearly separated in the groundwater level records, and their instantaneous frequencies can be confidently related with the semi-daily,

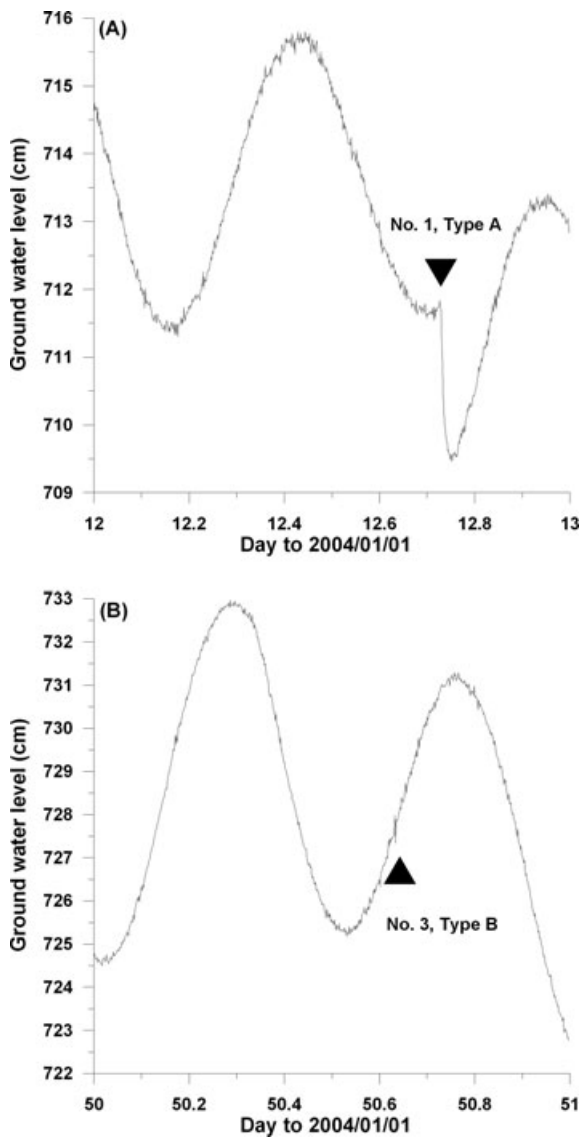


Figure 6. Type A and type B groundwater level anomalies at Hualien.

daily, semi-monthly, monthly tides without the input of barometric, precipitation and/or Earth tide information (Fig. 2). HHT<sub>3</sub> series that composed by every three observed points from original data provide a relatively fast and effective way to reduce the noise and stand out the coseismic signals (Figs 3–5). This technique may serve as a candidate for automation work in the earthquake monitoring involving large quantity of data series.

When IMFs are performed by EMD, the median of the instantaneous IMFs frequency should gradually decrease along with the increasing orders. However, we found that the median of the IMF<sub>3</sub> instantaneous frequency is larger than those of IMF<sub>1</sub> and IMF<sub>2</sub> in this study. This characteristic suggests that the energy involved in IMF<sub>3</sub> with the strong amplitude is contributed by earthquakes. In this study, type-A was detected in the groundwater level record for a temporal period longer than 6 min and positively related with the earthquake magnitude and hypocentre distance. For type-B, the groundwater level changes are generally less than 2 min, and the detection is strongly dependent on the resolution of recording time and propagation of the strong seismic waves. The HHT method provides a valuable tool for decomposing the groundwater level data

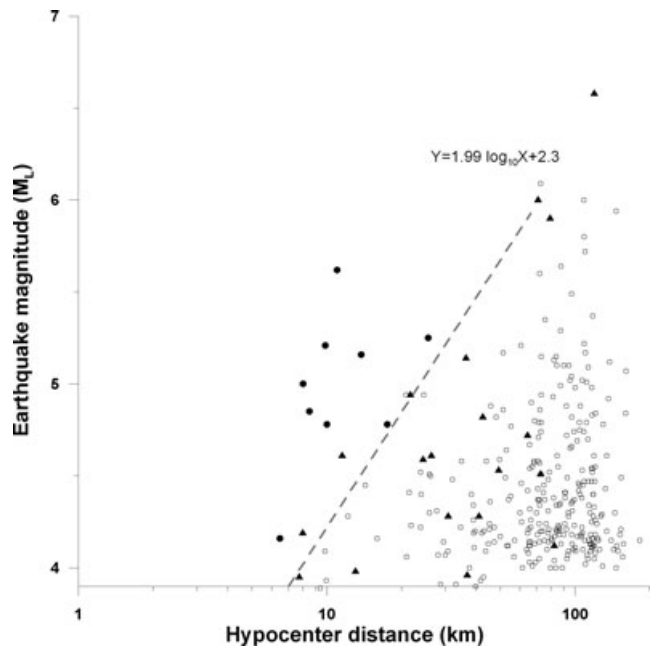


Figure 7. Earthquake magnitude versus hypocentre distance during the period from 2004 to 2006. The circle and triangle denote type-A and B in raw data, respectively. The opened circle shows earthquakes without coseismic signals. The dashed line represents the lower limit for 286 earthquakes ( $M_L \geq 3.95$ ; hypocentre distance  $\leq 120$  km) without coseismic signals.

through EMD process and obtaining the required coseismic signals in the IMFs results.

## ACKNOWLEDGMENTS

The authors would like to thank Dr W.C. Lai for providing the groundwater data of Hualien monitoring well through the authority of the Water Resources Agency of Taiwan. We also thank the Central Weather Bureau of Taiwan for providing the data of earthquake relocation and typhoons. The comments of three anonymous reviewers are greatly appreciated to improve our manuscript.

## REFERENCES

- Barnes, A.E., 1992. The calculation of instantaneous frequency and instantaneous bandwidth, *Geophysics*, **57**, 1520–1524.
- Bedrosian, E., 1963. A product theorem for Hilbert transform, *Proc. IEEE*, **51**, 868–869.
- Bredehoeft, J.D., 1967. Response of well-aquifer systems to Earth tides, *J. geophys. Res.*, **72**, 3075–3087.
- Brodsky, E.E., Roeloffs, E., Woodcock, E., Gall, I. & Manga, M., 2003. A mechanism for sustained groundwater pressure changes induced by distant earthquakes, *J. geophys. Res.*, **108**(B8), 2390, doi:10.1029/2002JB002321.
- Doan, M.L. & Cornet, F.H., 2007. Small pressure drop triggered near a fault by small teleseismic waves, *Earth planet. Sci. Lett.*, **258**, 207–218, doi:10.1016/j.epsl.2007.03.036.
- Hahn, S., 1996. *Hilbert Transform in Signal Processing*, Artech House, Norwood, MD, 442 pp.
- Ho, C.S., 1988. *An Introduction to the Geology of Taiwan*, 2nd edn, Central Geological Survey, The Ministry of Economic Affairs, Taipei, 192 pp.
- Huang, N.E. et al., 1998. The empirical mode decomposition and the Hilbert spectrum for nonlinear and non-stationary time series analysis, *Proc. R. Soc. Lond., Ser. A*, **454**, 903–995.

- Huang, N.E., Shen, Z., Long, S.R., Shen, S.S.P., Hsu, N.H., Xiong, D., Qu, W. & Gloersen, P., 2003. On the establishment of a confidence limit for the empirical mode decomposition and Hilbert spectral analysis, *Proc. R. Soc. Lond., Ser. A*, **459**, 2317–2345.
- Huang, N.E., Shen & Samuel, S.P. (Eds), 2005. *The Hilbert Huang Transform and its Application*, World Scientific Publishing Co. Pte. Ltd., Singapore, 311 pp.
- Igarashi, G. & Wakita, H., 1991. Tidal responses and earthquake-related changes in the water level of deep wells, *J. geophys. Res.*, **96**, 4269–4278.
- Kano, Y. & Yanagidani, T., 2006. Broadband hydroseismograms observed by closed borehole wells in the Kamioka mine, central Japan: response of pore pressure to seismic waves from 0.05 to 2 Hz, *J. geophys. Res.*, **111**, B03410, doi:10.1029/2005JB003656.
- Kitagawa, G. & Matsumoto, N., 1996. Detection of coseismic changes of underground water level, *J. Am. Stat. Assoc.*, **91**, 521–528.
- Matsumoto, N., 1992. Regression and analysis for anomalous changes of ground water level due to earthquakes, *Geophys. Res. Lett.*, **19**, 1193–1196.
- Matsumoto, N. & Roeloffs, E.A., 2003a. Hydrological response to earthquake in the Haibara well, central Japan: I. Groundwater level changes revealed using state space decomposition of atmospheric pressure, rainfall and tidal responses, *Geophys. J. Int.*, **155**, 885–898.
- Matsumoto, N. & Roeloffs, E.A., 2003b. Hydrological response to earthquake in the Haibara well, central Japan: II. Possible mechanism inferred from time-varying hydraulic properties, *Geophys. J. Int.*, **155**, 899–913.
- Montgomery, D.R. & Manga, M., 2003. Streamflow and water well responses to earthquakes, *Science*, **300**, 2047–2409, doi:10.1126/science.1082980.
- Narasimhan, T.N., Kanehiro, B.Y. & Witherspoon, P.A., 1984. Interpretation of Earth tide response of three deep, confined aquifer, *J. geophys. Res.*, **89**, 1913–1924.
- Quilty, E.G. & Roeloffs, E.A., 1991. Removal of barometric pressure response from water level data, *J. geophys. Res.*, **96**, 10209–10218.
- Quilty, E.G. & Roeloffs, E.A., 1997. Water level changes in response to the December 20, 1994 M4.7 earthquake near Parkfield, California, *Bull. seism. Soc. Am.*, **87**, 310–317.
- Roeloffs, E.A., 1988. Hydrologic precursors to earthquakes: a review, *Pure appl. Geophys.*, **126**, 177–206.
- Roeloffs, E.A., 1998. Persistent water level changes in a well near Parkfield, California, due to local and distant earthquakes, *J. geophys. Res.*, **93**, 13 619–13 634.
- Rojstaczer, S., 1988. Intermediate period response of water levels in wells to crustal strain: sensitivity and noise level, *J. geophys. Res.*, **93**, 13 619–13 634.
- Van Der Kamp, G. & Gale, J.E., 1983. Theory of Earth tide and barometric effects in porous formations with compressible grains, *Water Resour. Res.*, **19**, 538–544.